Electrodialytic Hydrogen Production and Critical Raw Materials Recovery from Secondary Resources

Joana Almeida *, Cátia Magro, Eduardo P. Mateus and Alexandra B. Ribeiro *

Center for Environmental and Sustainability Research, Department of Sciences and Environmental Engineering, School of Sciences and Technology, NOVA University Lisbon, Caparica Campus, 2829-516 Caparica, Portugal; c.magro@campus.fct.unl.pt (C.M.); epm@fct.unl.pt (E.P.M.)

* Correspondence: js.almeida@campus.fct.unl.pt (J.A.); abr@fct.unl.pt (A.B.R.)

Abstract: Electrodialytic technologies are defined as treatment processes that promote the removal/recovery of substances in a matrix, based on the application of low-level current intensities. Additionally, along these processes hydrogen is self-generated, allowing them to operationally produce clean energy. This energy carrier is produced due to electrolysis reactions occurring at the cathode end of the electrodialytic reactor, when using inert electrodes. Herein, hydrogen production during the electrodialytic treatment of sewage sludge and mining residues suspensions (coupled with effluent or sewage sludge), at 50 and 100 mA, was assessed. During the electrodialytic treatment of sewage sludge, hydrogen purity production achieved 33%. When effluent or sewage sludge were used as enhancements in mining residues suspensions, hydrogen purity reached 71% and 34%, respectively. Furthermore, a proton-exchange membrane fuel cell was connected to the cathode compartment of the electrodialytic reactor. The electrical energy generated from self-hydrogen produced at 100 mA achieved ≈1 V in all performed experiments. Simultaneously, critical raw materials extraction, namely phosphorus and tungsten, was evaluated. When the process was applied to mining residue suspensions combined with sewage sludge, the highest extraction ratio of phosphorus (71%) and tungsten (62%) was observed.

Keywords: electrodialytic technology; hydrogen production; proton-exchange membrane fuel cell; energy; phosphorus; tungsten

1. Introduction

Raw materials are crucial to the European Union's economy and, as the population grows [1], more resources are needed to meet the demand. Raw materials are the main base to produce a broad range of goods and applications for the quotidian life and modern technologies. However, the unhindered access to certain raw materials is raising awareness across the globe. Regarding the high economic importance and scarceness of certain raw materials, in 2017, the European Commission presented a list with 27 critical raw materials to emphasize the need to find reliable alternative suppliers [2].

Simultaneously, the targets presented by European Commission for the period of 2021 to 2030 also comply the reduction of greenhouse gas emissions in more than 40% (regarding 1990 levels) and energy efficiency improvements above 32.5% [3].

Seeking for technology developments on clean energy production through non-fossil resources, its storage and further uses called for new and integrated strategies [4]. Thus, coupling the recovery of critical raw materials from secondary resources with the empowerment of clean energy production will move towards circular economy principles [5].

Technologies based in the electrodialytic process have proved their potential to remove/recover a wide range of contaminants/substrates from environmental matrices [6–8]. Electrodialytic technologies consist on the application of a direct or alternate low-level current density (mA/cm²) and low potential gradient (V/cm), between a pair of electrodes. Herein, ion-exchange membranes allow a selective separation of cations and anions in concentrated electrolytes' solutions [9]. In this sense, electrodialytic technologies are being shaped for critical raw materials upturn, namely phosphorus (P) from sewage sludge [8] and tungsten (W) from secondary mining resources [10].

Treated effluent and sewage sludge are by-products from wastewater treatment plants (WWTP). Sewage sludge can be regarded as a secondary resource of critical raw materials, e.g., due to its high P content, when compared with effluent. However, treated effluent have also shown feasible reuses in building products [11] and irrigation purposes [12], making electrodialytic treatment also attractive. Sewage sludge can be applied in soil fertilization/remediation if a pre-treatment promotes a product with high quality standards. Moreover, sewage sludge can be used as an energy resource for power and heat by conventional/emerging technologies through the use of biogas and biofuels. The reuse of sewage sludge can, therefore, be economically appealing and sustainable, preventing its disposal as waste in landfills [13].

On the other hand, mining industries produce extremely high quantities of residues due to the low ore grade concentrates [14]. Additionally, the disposal of these residues in open pits can cause severe landscape issues and environmental deterioration. Located in the central region of Portugal, Panasqueira mine has been active for more than one century, representing one of the largest tin (Sn)— W deposits in Europe. Mining residues disposed in Panasqueira area can also be a source of critical raw material, although their low ore grade in W, from wolframite [15].

Despite of promising results in substances removal and separation from a wide range of solid and liquid environmental matrices, energy requirements for electro-based technologies operation are still one of the main operational drawbacks of these treatments. Regarding current low-carbon economy principles [16], this topic was addressed in a proof-of-concept work presented by Magro et al., 2019 [17]. The use of hydrogen produced during the electrodialytic process due to water electrolysis reactions was studied. The experimental reactor was coupled to a proton exchange membrane fuel cell (PEMFC), at the cathode end. Water was reduced to hydrogen gas, with purity levels up to 97% (mol/mol) and promoting the generation of ≈1 V electrical energy throughout the course of wastewater treatment. However, many factors may decrease hydrogen cleanliness, namely the typology of the process, the experimental matrix, and the presence of contaminants, involving competitive redox reactions at the electrodes (e.g., chlorine gas, metals deposition) [17].

Sewage sludge and mining residues suspensions have in common high disposal rates and critical raw materials contents, making them particularly attractive for electrodialytic technologies. Coupling the self-hydrogen production and exploitation with the recovery of P and W, may lead to the decrease of primary energy consumption while decreasing costs, particularly in a full-scale perspective. In addition, treated matrices may be further applied for different purposes, such as in the construction industry [11,18,19], promoting the much needed closed loop systems.

In the present work, the experimental set-up of a three-compartment electrodialytic reactor was operated at 100 and 50 mA, for 1 h and 2 h, respectively. The aim was to compare hydrogen production and purity rates during the electrodialytic treatment of effluent, sewage sludge, and mining residues suspensions, with or without sewage sludge and effluent enhancements. In parallel, the recovery of P and W from all matrices under treatment was assessed.

2. Materials and Methods

2.1. Materials

Secondary effluent (Lisbon, Portugal) and sewage sludge (Sesimbra, Portugal) samples were collected from the secondary clarifier of the respective wastewater treatment plants. Mining residues suspensions were prepared with a rejected fraction from the sludge circuit from Panasqueira mine (Covilhã, Portugal).

2.2. Experimental

The experimental set-up is presented on Figure 1. A three-compartment electrodialytic reactor acryl XT (RIAS A/S, Roskilde, Denmark), with an internal diameter of 80 mm and unitary compartment lengths of 50 mm was used. Anode and cathode compartments were separated from the central sector by an anion exchange membrane, AR204SZRA, MKIII, Blank (Ionics, Ringwood, NJ USA) and a cation exchange membrane, CR67, MKIII, Blank (Ionics, Ringwood, NJ, USA), respectively. Electrodes composition were Ti/MMO Permaskand wire, with a diameter of 3 mm and a length of 50 mm (Grønvold & Karnov A/S, Copenhagen, Denmark). A power supply E3612A (Hewlett Packard, Palo Alto, USA) was connected to the electrodialytic reactor for constant current. A magnetic stirrer was used in the central compartment to maintain the mixtures in suspension (Figure 1).
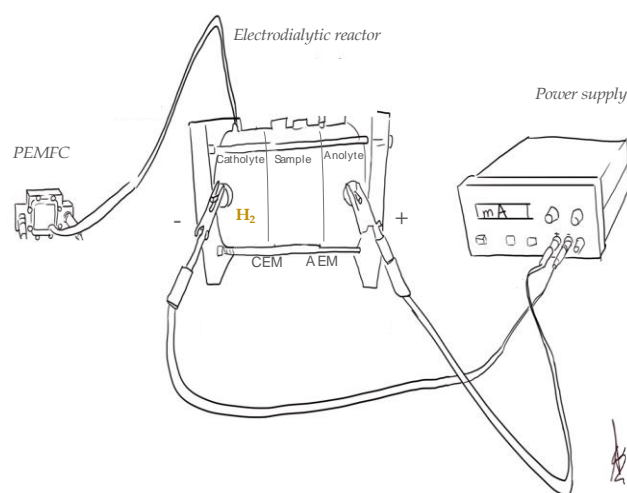
Figure 1. Schematic electrodialytic reactor coupled with a proton-exchange membrane fuel cell (PEMFC). CEM—Cation Exchange Membrane; AEMAnion—Exchange Membrane.

Sewage sludge tests were performed adding 200 mL of sample to the central compartment. Suspensions with effluent or sewage sludge and mining residues were prepared at the same L/S (9), adding 22.2 g of solid sample to 200 mL of liquid sample. Both anolyte and catholyte compartments were filled with 250 mL of 0.01 M $NaNO_3$.

Six electrodialytic experiments were carried out with three matrices and two current intensities (50 and 100 mA), in duplicate: Sewage sludge, mining residues with effluent, and mining residues with sewage sludge. The data from these experiments was compared with the effluent and mining residues data from [17], and ten electrodialytic experiments were evaluated (Table 1).

Table 1. Electrodialytic experiments conducted and used to compare gas capture and critical raw materials recovery.

Code	Operation Time (min)	Current Intensity (mA)	Matrix
E50 *	120	50	Effluent
E100 *	60	100	
SS50	120	50	Sewage Sludge
SS100	60	100	
MR50 *	120	50	Mining Residues and Briny Water
MR100 *	60	100	
MRE50	120	50	Mining Residues and Effluent
MRE100	60	100	
MRSS50	120	50	Mining Residues and Sewage Sludge
MRSS100	60	100	

E—Effluent; SS—Sewage sludge, MR—Mining residue. * Data from [17].

The hydrogen produced at the reactor cathode was collected in a storage cylinder with 30 mL of capacity (Horizon Fuel Cell Technologies, Singapore). The gas volume was measured every 10 min. For hydrogen purity analysis, the cathode compartment exit vent was connected to a 500 mL tedlar sample bag with a single polypropylene septum fitting (SKC, Cerritos, CA, USA) for 6 h. The gas was analyzed by Gas Chromatography with Thermal Conductivity Detector (GC-TCD). Finally, for electrical power generation, the cathode compartment was directly connected to a 32 mm × 32 mm × 10 mm PEMFC, with a nominal voltage of ≈1 V (Horizon Fuel Cell Technologies, Singapore).

The electrodialytic reactor and the fuel cell open circuit voltage were monitored every 10 min using a multimeter KT1000H (KIOTTO, Lisbon, Portugal) [17].

2.3. Methods

At the beginning and at the end of every electrodialytic experiment performed, pH and conductivity were measured in central and electrolytes compartments by means of pH (EDGE, HANNA, Providence, RI, USA) and conductivity meters (LAQUA twin, HORIBA Ltd., Kyoto, Japan).

Total concentrations of arsenic (As), calcium (Ca), cooper (Cu), potassium (K), magnesium (Mg), sodium (Na), P, sulfur (S), Sn, W and zinc (Zn) were determined by Inductively Coupled Plasma with Optical Emission Spectrometry (ICP-OES) (HORIBA Jobin-Yvon Ultima, Kyoto, Japan), equipped with generator RF (40.68 MHz), monochromator Czerny-Turner with 1.00 m (sequential), automatic sampler AS500 and dispositive CMA-Concomitant Metals Analyzer.

Sample preparation for elements´ quantification was performed through acid extraction of solid matrices (dried for 48 h at ≈20 °C): 0.5 g of solid sample with 9 mL HNO_3 (65%) and 3 mL HCl (37%) were placed on a shaking table at ≈125 rpm for 48 h. Finally, the samples were diluted in deionized water (1:25), filtered by vacuum through 0.45 μm MFV3 glass microfiber filters (Filter lab, Barcelona, Spain) and analyzed by ICP-OES.

Hydrogen purity was determined by GC-TCD on a Trace GC Ultra (Thermo Electron Corporation, Beverly, MA, USA), using a Carboxen 1010 plot column (0.32 mm of diameter, 30 m of length). The analytical process was performed in isothermal mode at 35 °C for 50 min. A gastight syringe (vici precision sampling, Baton Rouge, LA, USA) was used to inject a volume of 250 μL on the GC system. The injector was set at 200 °C and the detector/transfer line at 120 °C.

Data statistical analysis was performed with GraphPad Prism software (version 7.0e). The statistically significant differences between samples for 95% level of significance were assessed with ANOVA tests.

3. Results and Discussion

Table 2 presents the initial concentrations of elements in the studied effluent, sewage sludge, and mining residues.

Table 2. Initial characterization of elements in the studied matrices.

Element	Matrix		
	Effluent (mg/L) *	**Sewage Sludge (mg/L)**	**Mining Residues (mg/kg) ***
As	n.d.	0.06 ± 0.01	218.57 ± 132.31
Ca	51.74 ± 18.34	158.98 ± 48.21	91.11 ± 27.08
Cu	0.04 ± 0.00	1.90 ± 0.48	76.82 ± 39.30
K	47.80 ± 29.10	25.51 ± 1.30	n.d.
Mg	118.00 ± 137.17	14.87 ± 3.35	n.d.
Na	524.55 ± 532.55	23.63 ± 0.07	n.d.
S	84.89 ± 65.27 [a]	78.35 ± 17.45[b]	789.59 ± 214.13 [A,B]
Sn	n.d.	0.17 ± 0.04 [c]	1.95 ± 0.53 [C]
Zn	0.07 ± 0.06 [e]	7.20 ± 0.99 [E]	n.d.
Cl⁻	908.1 ± 1013.7	81 [#]	5.6 ± 2.3

* Data from [17]; n.d.—not detected. # Value provided by the wastewater treatment plants (WWTP). Statistical analysis performed through multiple comparisons at $p < 0.05$ (95% confidence interval). Data with capital letters are statistically significantly different from the data with the same lower-case letter.

3.1. Characterization of Electrodialytic Experiments

Table 3 presents the pH and conductivity values at the beginning and at the end of the electrodialytic experiments. As expected, the initial pH of the effluent (7.67 ± 0.16), sewage sludge (6.68 ± 0.02), and mining residues suspensions (4.57 ± 1.74) presented different levels. The combination of effluent or sewage sludge with mining residues (pH slightly acid), promoted the neutralization of the matrices (pH of 7.24 ± 0.12 and 7.18 ± 0.04, respectively). Sufficient conductivity on the media has to be guaranteed to assure the passage of the current, and consequently, the removal of elements. The effluent was the matrix with higher conductivity values (2.41 ± 2.12 mS/cm), enhancing the conductivity of mining residues when suspensions were mixed with effluent (from 1.82 ± 0.54 to 2.55 ± 1.92 mS/cm).

**Table 3.** Initial and final pH and conductivity values in the reactor compartments.

Experiment	Compartment	pH		Conductivity (mS/cm)	
		Initial	Final	Initial	Final
E50 *	Anode	6.46 ± 0.55	2.20 ± 0.02	0.90 ± 0.06	2.70 ± 0.00 [j]
	Cathode		12.21± 0.01 [a]		2.45 ± 0.2[l]
	Sample	7.67 ± 0.16	4.54 ± 2.55	2.41 ± 2.12	1.80 ± 0.86
E100 *	Anode	6.46 ± 0.55	2.21 ± 0.04	0.90 ± 0.06	2.85 ± 1.06 [k]
	Cathode		12.11 ± 0.01 [b]		1.94 ± 0.23
	Sample	7.67 ± 0.16	2.85 ± 0.20 [o]	2.41 ± 2.12	1.49 ± 0.15
SS50	Anode	7.54 ± 0.38	2.27 ± 0.19	0.54 ± 0.06	1.24 ± 0.14 [l]
	Cathode		11.77 ± 0.13 [A,c]		0.97 ± 0.02
	Sample	6.68 ± 0.02	5.96 ± 0.18	0.81 ± 0.02	0.37 ± 0.01
SS100	Anode	7.54 ± 0.38	2.15 ± 0.11	0.54 ± 0.06	0.94 ± 0.17 [K]
	Cathode		11.51 ± 0.08 [B,d]		1.06 ± 0.21
	Sample	6.68 ± 0.02	5.86 ± 0.14	0.81 ± 0.02	0.30 ± 0.01
MR50 *	Anode	6.46 ± 0.55	2.02 ± 0.11	0.90 ± 0.06	3.25 ± 0.21 [L]
	Cathode		12.30 ± 0.01 [C,e]		2.40 ± 0.14
	Sample	4.57 ± 1.74	5.91 ± 0.45	1.82 ± 0.54	1.41 ± 0.49
MR100*	Anode	6.46 ± 0.55	1.99 ± 0.04f	0.90 ± 0.06	2.55 ± 0.07
	Cathode		12.21 ± 0.25 [D,g]		2.08 ± 0.46
	Sample	4.57 ± 1.74	4.42 ± 1.33	1.82 ± 0.54	0.24 ± 0.16
MRE50	Anode	6.46 ± 0.55	2.00 ± 0.02	0.90 ± 0.06	2.70 ± 0.14 [n]
	Cathode		12.31 ± 0.02 [C,h]		2.12 ± 0.54
	Sample	7.24 ± 0.12	6.50 ± 0.22	2.55 ± 1.92	1.17 ± 0.60
MRE100	Anode	6.46 ± 0.55	2.08 ± 0.01	0.90 ± 0.06	4.00 ± 0.99
	Cathode		12.25 ± 0.03 [D,i]		2.20 ± 0.14
	Sample	7.24 ± 0.12	7.51 ± 0.12 [O]	2.55 ± 1.92	1.68 ± 0.32
MRSS50	Anode	7.54 ± 0.38	2.36 ± 0.11	0.54 ± 0.06	1.00 ± 0.50 [J,N]
	Cathode		11.65 ± 0.16 [A,E,H]		1.12 ± 0.28
	Sample	7.18 ± 0.04	6.38 ± 0.23	0.65 ± 0.01	0.61 ± 0.37
MRSS100	Anode	7.54 ± 0.38	2.47 ± 0.18 [F]	0.54 ± 0.06	1.05 ± 0.30 [K]
	Cathode		11.57 ± 0.11 [B,G,I]		0.91 ± 0.04 [M]
	Sample	7.18 ± 0.04	6.31 ± 0.01	0.65 ± 0.01	0.43 ± 0.01

E—Effluent; SS—Sewage sludge, MR—Mining residue. * Data from [17]. Statistical analysis performed through multiple comparisons at $p < 0.05$ (95% confidence interval). Data with capital letters are statistically significantly different from the data with the same lower-case letter.

After the electrodialytic process, almost all tested matrices turned slightly more acid (Table 3). This occurred due to the anion exchange membrane permselectivity, which allows the passage of H^+ to the sample compartment and, consequently, the pH tends to decrease. In the anode and cathode compartment, pH values reached ≈2 and ≈12, respectively. This was expected since water electrolysis promotes the generation of H^+ at the anode and OH^- at the cathode compartment. In addition, conductivity in the sample compartment decreased after the experiments, suggesting the electromigration of ions to the anolyte or to the catholyte.

The electrodialytic reactor voltage decreased along the time (Figure 2) and was faster during the experiments performed at 100 mA. Ohm's law defines an inverse relation between resistivity (or conductivity) and voltage, when current intensity is maintained constant. Thus, the increase in conductivity from 0.54/0.90 mS/cm to 0.94–4.0 mS/cm in the anolyte and to 0.91–2.5 mS/cm in the catholyte (Table 3) are related to the voltage decreased in the central compartment. The conductivity in the central compartment is dependent on the matrix and, since the matrices are highly heterogeneous, high standard deviations are observed to the parameters monitored. The experiments operated with sewage sludge and mining residues suspensions showed a voltage increase in the final minutes of the experiments (Figure 2). As an example, when sewage sludge experiments where conducted at 100 mA, the voltage inside the reactor decreased from ≈31 V to ≈25 V after 30 min and increased until ≈34 V in the following 30 min of experiment. The reduction of ions and the energy efficiency decrease related to ohmic losses may have contributed for the oscillations observed.
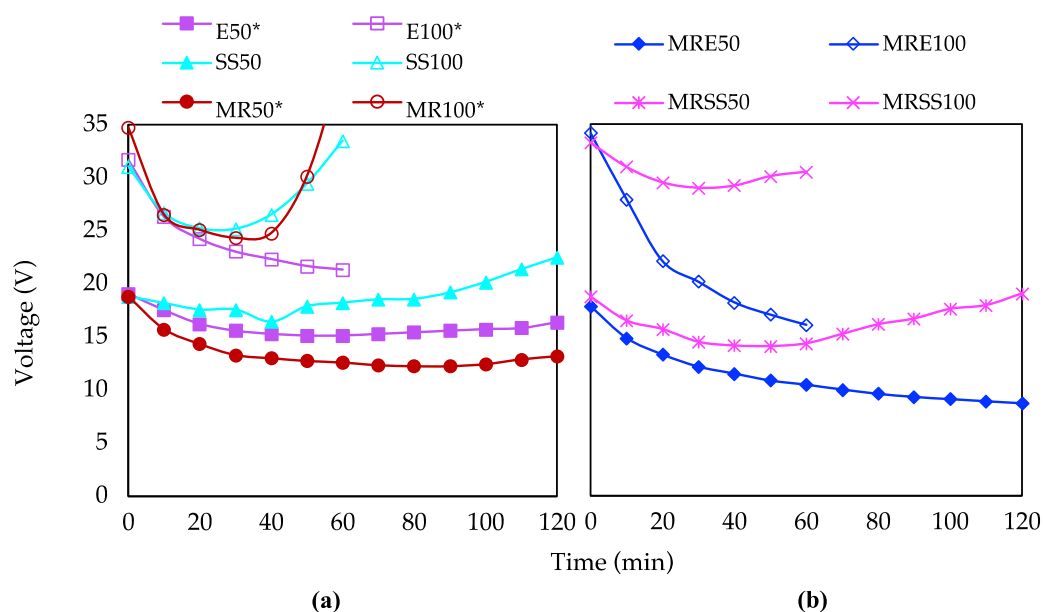
Figure 2. Voltage variation during the electrodialytic treatment: (**a**) effluent, sewage sludge, and mining residues suspensions; (**b**) mining residues suspensions with effluent or sewage sludge, at 50 and 100 mA. E—Effluent; SS—Sewage sludge, MR—Mining residue. *Data from [17].

3.2. Critical Raw Materials Extraction

Sewage sludge and used mining residues can be considered secondary resources of critical raw materials, namely for P and W, respectively. Table 4 presents the initial contents of P and W in all matrices and studied suspensions. Effluent has limited P contents (3.21 ± 0.04 mg/L) since standards for WWTP impose a P removal above 75% for further disposal [20]. On the other hand, sewage sludge is enriched in P (65.83 ± 19.60 mg/L). Additionally, the amount of P in mining residues (36.57 ± 18.74

mg/kg), could potentially be recovered when suspensions are prepared with sewage sludge (108.66 ± 38.34 mg/kg).

Table 4. Matrices' initial and final critical raw materials content, at 50 and 100 mA.

Experiment		Phosphorus		Tungsten	
		Initial	Final	Initial	Final
E50 *	mg/L	3.21 ± 0.04 [a]	2.84 ± 0.51 [b]	nd [#]	nd [#]
E100 *			3.30 ± 0.14 [c]		nd [#]
SS50	mg/L	65.83 ± 19.60	156.97 ± 30.73 [B,d]	nd [#]	nd [#]
SS100			146.83 ± 0.25 [C,e]		nd [#]
MR50 *	mg/kg	36.57 ± 18.74	20.73 ± 23.81 [D]	5.30 ± 1.56	5.64 ± 0.43 [f]
MR100 *			30.29 ± 4.88 [E]		4.88 ± 1.58 [g]
MRE50	mg/kg	39.80 ± 20.61	4.22 ± 0.64 [D]	5.30 ± 1.56	3.89 ± 0.13 [h]
MRE100			17.81 ± 22.15 [E]		3.76 ± 0.27
MRSS50	mg/kg	108.66 ± 38.34 [A]	29.59 ± 1.11 [D]	5.30 ± 1.56	1.71 ± 0.41 [F,H]
MRSS100			33.51 ± 0.66 [E]		1.63 ± 0.02 [G]

E—Effluent; SS—Sewage sludge, MR—Mining residue; * Data from [17]; [#] nd—not detected. Statistical analysis performed through multiple comparisons at $p < 0.05$ (95% confidence interval). Data with capital letters are statistically significantly different from the data with the same lower-case letter.

After the electrodialytic treatment, differences on the final content of P and W were observed (Table 4). Sewage sludge showed a higher P content after the experiments. Regarding phosphoric acid speciation, for pH of suspensions between 2 and 6, $H_2PO_4^-$ is dominant. When pH increases from 6 to 10, HPO_4^{2-} is the main specie present [21]. Thus, since pH turned to ≈6 in the central compartment at 50 and 100 mA, $H_2PO_4^-$ is the main form in the suspension, being P more available in the media and contributing for the increased P amount detected. Phosphorus availability can also be limited by iron and aluminum at acidic pH and calcium at alkaline pH [22]. Sewage sludge has 158.98 ± 48.21 mg/L of calcium (Table 2). When pH is above 5.5, phosphates can react with calcium to form calcium phosphates. Considering sewage sludge eventual contents on aluminum [23], when pH is below 5.5 it may react more readily with phosphates, reducing the amount of water-soluble P components while increasing the amount of insoluble aluminum phosphates [24].

On the other hand, when mining residues suspension were prepared with sewage sludge, there was a significant decrease of P in the final sample (≈32 mg W/kg; extraction ≈71%). P may form bonds with sulfur (phosphorous sulfides), chloride (phosphorus chloride) ions and calcium (calcium phosphates) [25]. Considering mining residues composition (Table 2), there are high contents of sulfur (789.6 ± 214.1 mg/kg) and, in lower quantities, chloride (5.6 ± 2.3 mg/kg). The formation of other chemical species and the removal of Al, Ca and Fe by the electrodialytic process may had promoted the solubilization of P and increased P extraction/removal from the sample inside the reactor central compartment.

Mining residues have tungsten in the form of (Fe, Mn) WO_4 (wolframite), and contents of W (5.30 ± 1.56 mg/kg). When mining residues suspension were electrodialytic treated with briny water [17], the extraction of W was not significant for both current intensities applied: 5.64 ± 0.43 at 50 mA and 4.88 ± 1.58 mg/kg at 100 mA (Table 4). Monomeric tungstate ion is only stable in neutral/alkaline solutions (pH > 6.2), which may explain the differences of dissolved tungsten concentrations [26].
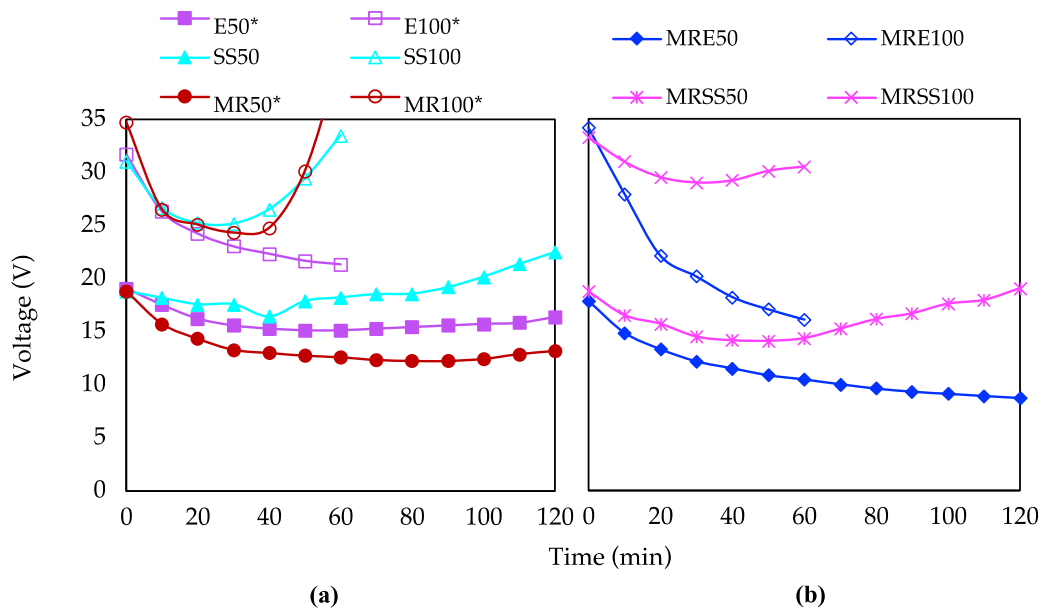
Contrarily, when mining residues suspensions were prepared with effluent, the extraction of W was higher, meaning lower contents of W in the final sample (≈4 mg W/kg; extraction ≈25%). This may have occurred due to complex formation, which promotes the extraction of W from mining residues. Effluent is rich in calcium (Table 2), where W can form complexes such as $CaWO_4$ [27]. When mining residues suspensions were mixed with sewage sludge, W extraction showed the highest extraction rate. Less than ≈2 mg/kg of W (W extraction ≈62%) remained in the final sample

(Table 4), which may be caused due to W complexes formation with P (tungsten phosphides, WP) together with W calcium complexes [28].

Coupling mining residues with effluent and sewage sludge promoted a final pH range of the suspension ≈6.3–7.5. In the absence of complexing substances, W in aqueous solution mainly exists under the soluble form of tungstic ions $(WO_4)^{2-}$ that are stable at neutral and alkaline pH (higher solubility at alkaline pH). The W insoluble/slightly soluble species WO_2 and W_2O_5 are stable between pH 5 and 6.5, while WO_3 is stable below pH 5 throughout all the oxidizing conditions [29,30].

3.3. Hydrogen Generation and Purity

Figure 3 presents the gas produced at the cathode compartment during the electrodialytic experiments. A maximum of 30 mL was collected in all experiments due to the reservoir capacity. The hydrogen flow rate production during electrodialytic treatments can be affected by the matrix itself, competing cathode reactions, and the current intensity applied [17].

Figure 3. Gas collected during the electrodialytic treatment from the cathode compartment: (**a**) effluent, sewage sludge, and mining residues suspensions at 50 and 100 mA; (**b**) mining residues suspensions with effluent or sewage sludge, at 50 and 100 mA. E—Effluent; SS—Sewage sludge, MR—Mining residue. * Data from [17].

At 100 mA, effluent, sewage sludge, and mining residues with or without wastewater resources, showed similar rates of gas production (≈1 mL/min). However, at 50 mA, the gas production rates were lower and more variable, from a minimum of 0.33 mL/min on sewage sludge compared to a maximum of 0.68 mL/min on effluent [17] (Table 5).

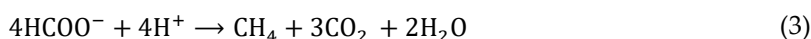**Table 5.** Hydrogen flow rate (slope), its R-square and purity.

Experiment	Hydrogen		
	Flow mL/min (Slope)	R-Square (Slope)	Purity *w/w* (%)
E50 *	0.68	0.97	-
E100 *	1.13	0.96	90.4 ± 0.3 [a]
SS50	0.33	0.97	-
SS100	1.02	0.94	32.6 ± 0.5 [b]
MR50 *	0.62	0.94	-
MR100 *	1.12	0.97	72.4 ± 0.7 [A,B]
MRE50	0.47	0.91	-
MRE100	1.05	0.96	71.3 ± 0.7 [A,B,c]
MRSS50	0.50	0.94	-
MRSS100	1.0	0.93	33.6 ± 4.9 [A,B,C]

E—Effluent; SS—Sewage sludge, MR—Mining residue; * Data from [17]. Statistical analysis performed through multiple comparisons at $p < 0.05$ (95% confidence interval). Data with capital letters are statistically significantly different from the data with the same lower-case letter.

The gas from the cathode compartment was collected in tedlar sample bags and analyzed. Table 5 shows the hydrogen purity for the experiments performed at 100 mA. Comparing the results from the previous work [17], where the highest hydrogen purity (% *w/w*) was verified during effluent electrodialytic treatment (90.4 ± 0.3%), in the present study sewage sludge reported the lowest hydrogen purity (32.6 ± 0.5%). Effluent hydrogen purity has statistically significant differences ($p < 0.05$) from all the experiments, except from sewage sludge. Moreover, mining residue suspensions with sewage sludge or effluent are statistically significant different between them.

The hydrogen production rate and purity may have been affected due to competing cathode reactions. Comparing effluent and mining residues, sewage sludge is richer in organic matter [31]. Hydrogen production may be affected by methane (CH_4), which is produced by methanogenic organisms commonly present in most of mixed cultures. Hydrogenotrophic organisms may transform CO_2 and H_2 to produce methane gas [32] (Equation (1)). Bacteria may move together through direct current application by electroosmosis and electrophoresis phenomena [33]. Furthermore, some bacteria may adhere to several surfaces or other microorganism [34], promoting also their movement to the cathode compartment. Microorganisms form clusters, due to their natural behavior and may interact with environment in experimental conditions [35].

Hydrolysis and fermentation reactions may also lead to the generation of CH_4 and CO_2 gases in the reactor (Equations (2) and (3)) [36]. Sewage sludge have also nitrogen contents (total nitrogen = 500 mg/L, data provided by the WWTP). This may have contributed for NO_2 gas generation [17] (Equation (4)), decreasing the purity of the hydrogen collected.

$$4H_2 + CO_2 \longrightarrow CH_4 + H_2O \tag{1}$$

$$CH_3COO^- + H^+ \longrightarrow CH_4 + CO_2 \tag{2}$$

$$4HCOO^- + 4H^+ \longrightarrow CH_4 + 3CO_2 + 2H_2O \tag{3}$$

$$NO_2 + H_2O \longrightarrow NO_3^- + 2H^+ \tag{4}$$

Considering hydrogen capture conditions at 1 atm and 25 °C and comparing with [17] results at 100 mA, the hydrogen purity collected from each matrix decreased in the following sequence: E100 > MR100 > MRE100 > MRSS100 > SS100 (Table 5).

3.4. Electrical Requirements and Savings

Electrodialytic experiments were carried out at a constant current of 50 and 100 mA. Thus, the electrical energy required during each process, regarding the energy applied by the direct current

power source, was determined by Equation (5), where *I* is the current intensity (mA) and $V_{reactor}$ is the voltage inside the electrodialytic reactor (*V*), between the initial (t_0) and final (*t*) operation time (min):

$$E = I \int_{t_0}^{t} V_{reactor}(t) \, dt \qquad (5)$$

Electrical energy requirements grow with the increase of electrical current applied, considering the same circulated charge. The experiments performed at 100 mA required 9.5 ± 1.5 kJ of electrical energy and the experiments carried out at 50 mA required 5.50 ± 1.40 kJ.

Considering a H_2 heat of combustion of 141.8 MJ kg^{-1}, and fuel cell energy conversion efficiencies of 40–60% [37,38], between ≈5 to 8% of the electrical energy required in experiment MRE50 (the best case reported) can be saved. This may also translate into economic benefits on the overall electrodialytic treatment.

When the electrodialytic treatment is applied to liquid matrices, the energy requirements for the electrolysis reactions are lower due to associated higher conductivity values. On the other hand, in solid porous matrices, the electrodialytic process reaches higher voltage gradients due to the lower conductivity, requiring longer treatments. Coupling fuel cell technologies may be a key factor in electrodialytic energy savings, through the improvement on operation and energy efficiencies. In addition, self-hydrogen produced in electrodialytic reactors can be stored and used/sold for energy dependent industrial sectors.

In this sense, a proton-exchange membrane fuel cell (PEMFC) was connected directly to the cathode compartment from all the experiments carried out at 100 mA. The PEMFC initial open circuit voltage was between 1.2–1.4 V, showing a pronounced decrease in the first 10 min and remaining stable until the end of the experiments (Figure 4). In all cases, chemical energy was converted to electrical energy, supporting the versatility of PEMFC applicability to a broad range of matrices. Although PEMFC chemical energy transformation into electrical energy is not directly dependent on hydrogen quality, it may have repercussions on future PEMFC performance and long-term stability. Impurities in the gas that flows inside the PEMFC, such as CO, H_2S, NH_3, and CH_4, could cause damage on electrodes, catalyst poisoning and, consequently, fuel cell functioning degradation [39].
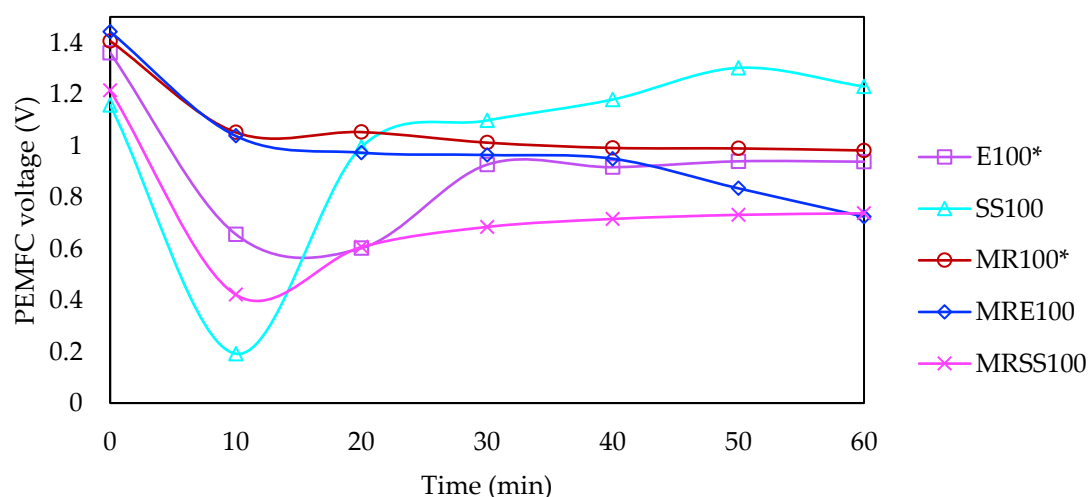
Figure 4. Proton-exchange membrane fuel cell voltage variation. E—Effluent; SS—Sewage sludge, MR—Mining residue. * Data from [17].

4. Conclusions

The present study proved the suitability of wastewater resources, as secondary effluent and sewage sludge, to enhance electrodialytic critical raw materials recovery from mining residues. Simultaneously, clean energy production was addressed due to the self-hydrogen generated during the electroremediation of the environmental matrices.

The electrodialytic extraction of P (71%) and W (62%) from sewage sludge and mining residues suspensions was more effective when both matrices were combined. This can potentiate circular economy while mitigating environmental negative impacts of waste disposal from both sewage sludge and mining industries.

Regarding the potential of electrodialytic technologies as hydrogen sources, the experiments performed demonstrated that hydrogen was produced in all tested cases, with purities between 33% (sewage sludge) and 71% (mining residues suspension with effluent). Competitive cathode reactions may affected the hydrogen purity, namely in sewage sludge due to its complex composition. Thus, future works should address the composition of other gases to verify competitive cathode reactions. Self-hydrogen produced during electroremediation of the matrices promotes a stable electrical energy generation (1.2–1.4 V) and a way to reuse the previous energy recovered. This was validated through a proton-exchange membrane fuel cell connected to the cathode compartment of the electrodialytic reactor. Hydrogen generated at cathode electrolysis reaction can reduce electrical energy requirements from 5% to 8%, namely in terms of electrodialytic treatments or other remediation strategies concerning electrochemically induced transport.

The critical raw materials recovered and the energy achievements may empower the sustainable growth of electrodialytic technologies, as these technologies can couple economic benefits.

References.

1. Eurostat Statistics Explained People in the EU-population Projections. Available online: https://ec.europa.eu/eurostat/statistics-explained/index.php?title=People_in_the_EU_-_population_projections#Population_projections (accessed on 13 April 2020).
2. European Comission. *Communication from the Comission to the European Parliament, the Council, the European Economic and Social Committee and the Committee of the Regions on the 2017 list of Critical Raw Materials for the EU*; European Comission: Brussels, Belgium, 2017.
3. European Commission. *2030 Climate and Energy Policy Framework*; European Commission: Brussels, Belgium, 2014.
4. Hart, P.S.; Feldman, L. Would it be better to not talk about climate change? The impact of climate change and air pollution frames on support for regulating power plant emissions. *J. Environ. Psychol.* **2018**, *60*, 1–8.
5. European Commission. *Communication from the Comission to the European Parliament, the Council, the European Economic and Social Committee and the Committee of the Regions-Closing the Loop-An EU Action Plan for the Circular Economy*; European Commission: Brussels, Belgium, 2015.
6. Ribeiro, A.B.; Mateus, E.P.; Ottosen, L.M.; Bech-Nielsen, G. Electrodialytic removal of Cu, Cr, and As from chromated copper arsenate-treated timber waste. *Environ. Sci. Technol.* **2000**, *34*, 784–788.
7. Magro, C.C.; Guedes, P.R.; Kirkelund, G.M.; Jensen, P.E.; Ottosen, L.M.; Ribeiro, A.B. Incorporation of different fly ashes from mswi as substitute for cement in mortar: An overview of the suitability of

electrodialytic pre-treatment. In *Electrokinetics Across Disciplines and Continents*; Ribeiro, A.B., Mateus, E.P., Couto, N., Eds.; Springer International Publishing: Cham, Switzerland, 2016; pp. 225–247; ISBN 9783319201795.

8. Guedes, P.; Mateus, E.; Almeida, J.; Ferreira, A.; Couto, N.; Ribeiro, A. Electrodialytic treatment of sewage sludge: Current intensity influence on phosphorus recovery and organic contaminants removal. *Chem. Eng. J.* **2016**, *306*, 1058–1066.

9. Ribeiro, A.B.; Mateus, E.P.; Couto, N. (Eds) *Electrokinetics across disciplines and continents: New strategies for sustainable development*; Springer International Publishing: Berlin/Heidelberg, Germany, 2016; 427 p; ISBN 9783319201795.

10. Almeida, J.; Craveiro, R.; Faria, P.; Silva, A.S.; Mateus, E.P.; Barreiros, S.; Paiva, A.; Ribeiro, A.B. Electrodialytic removal of tungsten and arsenic from secondary mine resources—Deep eutectic solvents enhancement. *Sci. Total Environ.* **2020**, *710*, 136364.

11. Magro, C.; Paz-Garcia, J.M.; Ottosen, L.M.; Mateus, E.P.; Ribeiro, A.B. Sustainability of construction materials: Electrodialytic technology as a tool for mortars production. *J. Hazard. Mater.* **2019**, *363*, 421–427.

12. Ferreira, A.R.; Couto, N.; Guedes, P.; Pinto, J.; Mateus, E.P.; Ribeiro, A.B. Electrodialytic 2-compartment cells for emerging organic contaminants removal from effluent. *J. Hazard. Mater.* **2018**, *358*, 467–474.

13. Kacprzak, M.; Neczaj, E.; Fijałkowski, K.; Grobelak, A.; Grosser, A.; Worwag, M.; Rorat, A.; Brattebo, H.; Almås, Å.; Singh, B.R. Sewage sludge disposal strategies for sustainable development. *Environ. Res.* **2017**, *156*, 39–46.

14. Schmidt, S.; Berghau, W.; Hutten, A. From deposit to concentrate : The basics of tungsten mining Part 1: Project generation and project development. *Int. Tungsten Ind. Assoc.* **2012**, *4*, 1–20.

15. Candeias, C.; Melo, R.; Ávila, P.F.; Ferreira da Silva, E.; Salgueiro, A.R.; Teixeira, J.P. Heavy metal pollution in mine-soil-plant system in S. Francisco de Assis-Panasqueira mine (Portugal). *Appl. Geochem.* **2014**, *44*, 12–26.

16. Ganiyu, S.O.; Martínez-Huitle, C.A.; Rodrigo, M.A. Renewable energies driven electrochemical wastewater/soil decontamination technologies: A critical review of fundamental concepts and applications. *Appl. Catal. B Environ.* **2020**, *270*, 118857.

17. Magro, C.; Almeida, J.; Paz-Garcia, J.M.; Mateus, E.P.; Ribeiro, A.B. Exploring hydrogen production for self-energy generation in electroremediation: A proof of concept. *Appl. Energy* **2019**, *255*, 113839.

18. Kappel, A.; Ottosen, L.M.; Kirkelund, G.M. Colour, compressive strength and workability of mortars with an iron rich sewage sludge ash. *Constr. Build. Mater.* **2017**, *157*, 1199–1205.

19. Almeida, J.; Ribeiro, A.B.; Silva, A.S.; Faria, P. Overview of mining residues incorporation in construction materials and barriers for full-scale application. *J. Build. Eng.* **2020**, *29*, 101215.

20. Diário da República. *Decreto-Lei n.º 152/2017 de 7 de Dezembro*; Diário da República: Lisbon, Portugal, 2017;.

21. Ugilt Sø, H. *Adsorption of Arsenic and Phosphate onto the Surface of Calcite as Revealed by Batch Experiments and Surface Complexation Modelling*; Technical University of Denmark: Lyngby, Denmark, 2011.

22. Goreau, T.J.; Larson, R.W.; Campe, J. Geotherapy: Innovative methods of soil fertility restoration, carbon sequestration, and reversing CO_2 increase. *Choice Rev. Online* **2015**, *53*, 1302.

23. Petzet, S.; Peplinski, B.; Bodkhe, S.Y.; Cornel, P. Recovery of phosphorus and aluminium from sewage sludge ash by a new wet chemical elution process (SESAL-Phos-recovery process). *Water Sci. Technol.* **2011**, *64*, 693–699.

24. Mackenzie, A.F.; Amer, S.A. Reactions of iron, aluminum and calcium phosphates in six Ontario soils. *Plant Soil* **1964**, *21*, 17–25.

25. Kouzbour, S.; Gourich, B.; Gros, F.; Vial, C.; Allam, F.; Stiriba, Y. Comparative analysis of industrial processes for cadmium removal from phosphoric acid: A review. *Hydrometallurgy* **2019**, *188*, 222–247.

26. Dermatas, D.; Braida, W.; Christodoulatos, C.; Strigul, N.; Panikov, N.; Los, M.; Larson, S. Solubility, sorption, and soil respiration effects of tungsten and tungsten alloys. *Environ. Forensics* **2004**, *5*, 5–13.

27. Wang, S.; Gao, H.; Sun, G.; Li, Y.; Wang, Y.; Liu, H.; Chen, C.; Yang, L. Structure characterization, optical and photoluminescence properties of scheelite-type $CaWO_4$ nanophosphors: Effects of calcination temperature and carbon skeleton. *Opt. Mater.* **2020**, *99*, 109562.

28. Miyazaki, H.; Nose, A.; Suzuki, H.; Ota, T. Phosphorus solid solution effects of electric and dielectric properties on sintered WO_3 ceramics. *J. Ceram. Soc. Jpn.* **2011**, *8*, 650–653.

29. Anik, M. pH-dependent anodic reaction behavior of tungsten in acidic phosphate solutions. *Electrochim. Acta* **2009**, *54*, 3943–3951.

30. Deltombe, E.; De Zoubov, N.; Pourbaix, M. Tungsten. In *Atlas of Electrochemical Equilibria in-Aqueous Solutions*; Pourbaix, M., Ed.; NACE: Houston, TX, USA, 1974; pp. 280–285.

31. Guedes, P.; Couto, N.; Almeida, J.; Rodrigues, A.M.; Mateus, E.P.; Ribeiro, A.B. Electrodialytic treatment of sewage sludge: Influence on microbiological community. *Int. J. Environ. Sci. Technol.* **2018**, *15*, 1103–1112.

32. Rivera, I.; Schröder, U.; Patil, S.A. Microbial electrolysis for biohydrogen production. In *Microbial Electrochemical Technology*; Elsevier: Amsterdam, The Netherlands, 2019; pp. 871–898.

33. Li, P.C.H.; Harrison, D.J. Transport, manipulation, and reaction of biological cells on-chip using electrokinetic effects. *Anal. Chem.* **1997**, *69*, 1564–1566.

34. Gill, R.T.; Harbottle, M.J.; Smith, J.W.N.; Thornton, S.F. Electrokinetic-enhanced bioremediation of organic contaminants: A review of processes and environmental applications. *Chemosphere* **2014**, *107*, 31–42.

35. Szumski, M.; Kłodzińska, E.; Buszewski, B. Separation of microorganisms using electromigration techniques. *J. Chromatogr. A* **2005**, *1084*, 186–193.

36. Ebbers, B.; Ottosen, L.M.; Jensen, P.E. Electrodialytic treatment of municipal wastewater and sludge for the removal of heavy metals and recovery of phosphorus. *Electrochim. Acta* **2015**, *181*, 90–99.

37. Salameh, Z. Energy storage. In *Renewable Energy System Design*; Elsevier: Amsterdam, The Netherlands, 2014; pp. 201–298; ISBN 9780123749918.

38. Staffell, I.; Green, R.; Kendall, K. Cost targets for domestic fuel cell CHP. *J. Power Sources* **2008**, *181*, 339–349.

39. Seo, J.G.; Kwon, J.T.; Kim, J.; Kim, W.S.; Jung, J.T. Impurity effect on proton exchange membrane fuel cell. In *Proceedings of the 2007 International Forum on Strategic Technology*; IFOST: Ulsan, Korea; 2007; pp. 484–487.